# PRECISE CALIBRATION OF MULTI-SEGMENT MANEUVERS FOR EUMETSAT POLAR SYSTEM (EPS) OPERATIONS PLANNING

**Yoke T. Yoon**(1), **Pier Luigi Righetti**(2)
(1)*PosiTim U.G. at EUMETSAT, Eumetsat-Allee 1, D-64295 Darmstadt, Germany, +49(0)6151-807 7, Yoke.Yoon@eumetsat.int*
(2)*EUMETSAT, Eumetsat-Allee 1, D-64295 Darmstadt, Germany, +49(0)6151-807 7, PierLuigi.Righetti@eumetsat.int*

***Abstract:*** *An observed discrepancy in the acceleration contribution from the out-of-plane (OOP) maneuver calibration of the Metop-B satellite has instigated a detail study that involves the reconstruction of the attitude model and thrust segments for precise maneuver calibration. The reconstruction and refinement of the models are based on telemetry values extracted from the Flight Dynamics system. A typical OOP maneuver for Metop satellites comprises a slew, a main thrust, and an anti-slew maneuver. Since the beginning of the Metop-A mission, the OOP maneuvers have been calibrated without accurate attitude knowledge in the POD. The main OOP thrust estimate obtained is sufficient for operations planning and the expected acceleration contribution from the slew and anti-slew maneuvers agrees closely to the theoretical values. In the case for Metop-B, an unexpected anomaly in the along-track acceleration contribution was observed in the two most recent OOP maneuvers. In view of that, a detailed attitude and thrust models during the OOP maneuver is reconstructed based on information retrieved from the spacecraft telemetry. The refined attitude model is used in the POD to help improve the calibration of each segment of the maneuver to better understand the cause of the discrepancy.*

***Keywords:*** *Maneuver Calibration, Precise Orbit Determination, GPS, Flight Dynamics*

## 1. Introduction

The EUMETSAT Polar System (EPS) comprises a series of three polar orbiting meteorological satellites, Metop, and is the European contribution to the EUMETSAT/NOAA Initial Joint Polar System (IJPS) in providing “morning” service for operational meteorology. Within the European framework, the Metop program is a joint undertaking between the European Space Agency (ESA) and EUMETSAT in which EUMETSAT is responsible for the development and operations of the ground segment, and routine operation of the space segment. Two of the three Metop satellites are currently in orbit with Metop-A close to its end-of-life operation. The three satellites are foreseen to provide polar data for climate monitoring over a minimum period of 14 years.

The Metop satellite is designed to fly in a sun-synchronous orbit with the local time at the descending node occurring at 09:30 ± 2 minutes and a repeat cycle of 29 days. In satisfying the scientific requirements for optimum observation collection, the ground track is kept within a dead band of ±5 km with respect to the reference and the frozen eccentricity condition is maintained. The orbit maintenance of Metop consists of three types of maneuver: short in-plane (SIP), long in-plane (LIP) and out-of-plane (OOP). In-plane (IP) maneuvers are considered short if the burn duration is less than 30 seconds at the beginning of life and less than 1 minute at the end of life. All SIP maneuvers are performed in the yaw-steering attitude pointing mode (YSM) whereas the LIP and OOP maneuvers are in fine pointing attitude mode (FPM) or geocentric mode (GEO).

In order to accurately characterize the in-orbit thruster performance for planning of future operations, maneuver calibration is performed in the precise orbit determination (POD) using GPS observations collected by the GNSS Receiver for Atmospheric Sounding (GRAS) instrument onboard Metop. GRAS provides dual frequency navigation and occultation observations for precise positioning and atmospheric sounding, respectively. In view of the ground and space segment operational conditions and limitations, precise maneuver calibration of the Metop satellites is not a straight forward process. One of the crucial knowledge required in the POD for precise maneuver calibration is the availability of accurate spacecraft pointing information throughout the duration of the maneuver, and the maneuver times and duration. For Metop, the attitude information can be acquired through post-processing of the spacecraft telemetry data. Reconstruction of the attitude knowledge on ground without telemetry data is not possible for the OOP maneuvers as part of the multi-segment burn is automatically commanded by the onboard Attitude and Orbit Control System (AOCS).

For IP maneuvers, the onboard AOCS activates a series of small thruster pulses to correct for the attitude pointing after the main burn. These pulses typically last for approximately 2-6 minutes and their impact cannot be neglected for short IP maneuvers. The profile of the pulses for each segment is extracted from the spacecraft telemetry data and then modeled as a single continuous thrust in the POD process. On the other hand, the OOP maneuver comprises five thrusting phases; start slew, stop slew, main burn, start anti-slew and stop anti-slew. The slew and anti-slew maneuvers are also performed by thrusters and the by-product of the IP acceleration contribution is taken into account in planning the OOP maneuver.

Since the beginning of the Metop-A mission, the OOP maneuvers have been calibrated without accurate attitude knowledge in the POD. The main OOP thrust estimate obtained is sufficient for operations planning and the IP acceleration contribution from the slew and anti-slew has stayed close to the theoretical values. Thus there was never a need for highly accurate calibration of each segment of the maneuvers for routine flight dynamics operations. However, in the last two OOP maneuvers for Metop-B an unexpected along-track acceleration bias has been observed in the POD that is never seen on Metop-A. Given the situation and the need to better understand the thruster performance of Metop-B, the necessity to refine the dynamic modeling for more accurate calibration of the multi-segment OOP maneuver arises.

The calibrated SIP maneuvers with stabilization phase information have thus far helped improve maneuver planning for orbit maintenance since 2012. The LIP maneuvers have been calibrated as a single thrust segment in the POD without accounting for the aftermath stabilization phase. The magnitude and duration of the thrust from the stabilization phase are significantly smaller than the LIP maneuver and is therefore neglected. It is foreseen that the effort to establish the capability to accurately calibrate multi-segment OOP maneuver for Metop-B will help resolve the along-track acceleration bias anomaly besides it being highly beneficial for future OOP maneuver planning especially for Metop-C and the EPS-Second Generation (SG).

The following sections of this paper present an overview of the Metop spacecraft characteristics, the maneuver segments and attitude profile reconstruction based on spacecraft telemetry, and the outcome of the multi-segment maneuver calibration performance from the POD. In conclusion, a short discussion will be included that relates the results to the thruster performance, improvements that can be implemented in the near future as well as the importance of this work for flight dynamics routine operations, and for future EPS and EPS-SG operations planning.

## 2. Overview of Metop Spacecraft Characteristics

### 2.1. Propulsion Subsystem

The Metop spacecraft is three-axis stabilized whereby the onboard AOCS is responsible for the automatic 3-axes attitude control. The orbit is controlled by thrust impulses as provided by the propulsion subsystem. This subsystem consists of four independent monopropellant hydrazine pressurized tanks that are coupled in pairs [1]. Each pair comprises eight thrusters. During normal operations, both tank pairs are in used.

As for the thrusters, they are mounted in pairs and are positioned on propulsion plates located on the spacecraft +/-Y and +/-Z faces to meet system level thrust/torque requirements [1]. They are tagged by numbers and each has its function to provide the necessary torque and thrust. Table 1 shows a summary of the thruster configuration and its corresponding function. In executing the OOP maneuver, thrusters T13 and T15 are used together to provide the necessary combined thrust in the +Y direction while keeping the torque balanced. However imbalance in the torque can occur during the propulsion phase as the spacecraft center of mass changes. Thrusters T7 and T9 are commonly used for IP maneuvers to provide the necessary thrust in the flight direction. These pairs of thrusters are the so-called propulsion thrusters. For the slew and anti-slew maneuvers, either the +Z/±Y or –Z//±Y thrusters are activated together to provide the necessary torque to rotate the spacecraft. These are the coupled thrusters. The four single thrusters provide the necessary torque on the spacecraft to stabilize the attitude pointing as commanded by the AOCS, and these are the attitude control thrusters. At times, the coupled thrusters are also used for attitude control.

**Table 1. Thruster module configuration and function**

| Thruster No. | | Thruster Function | |
|---|---|---|---|
| Prime | Redundant | Torque | Thrust |
| 1 | 2 | +Y | |
| 3 | 4 | -Y | |
| 5 | 6 | -X | |
| 7 | 8 | -Z | -Y |
| 9 | 10 | +Z | -Y |
| 11 | 12 | +X | |
| 13 | 14 | +Z | +Y |
| 15 | 16 | -Z | +Y |

The eight thrusters shown in Tab. 1 allows the generation of torque in all three axis and of propulsion in the ±Y axis. A graphical view of the thruster pair configuration is given in Fig. 1. The Cartesian reference frame indicated in the figure depicts the Metop satellite body frame of reference in which –Z points toward the Earth center. All the eight thruster configurations as described in Tab. 1 are shown in detailed in Fig. 1. The rectangular box on the left in Fig. 1 is a rough representation of the Metop spacecraft that complements the thruster configuration schematics on its right. The green patches signify the location of the thruster pairs grouping on the spacecraft.

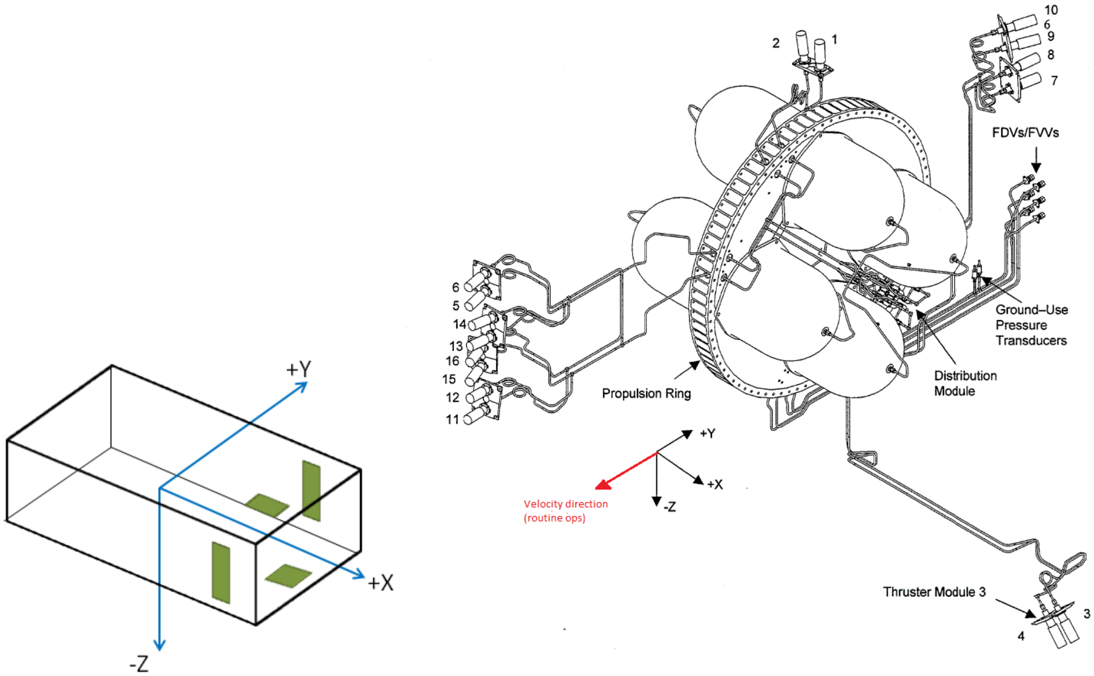


**Figure 1 Metop thruster configuration and location**

Each thruster is designed to deliver a nominal thrust of 22.7N at the beginning of life [1]. Currently, each thruster on Metop-B is providing on average 17.5N of thrust. The thrust provided is in the form of pulses and are designed to operate at 8 Hz. During the propulsion phase, the imbalance in the torque due to changes in the center of mass will cause one of the propulsion thrusters to pulsate less than the other. A similar imbalance in the torque and thrust applies to the slew and anti-slew maneuvers as well. Throughout the maneuver phase, the attitude control thrusters are actively controlled by the AOCS to correct the attitude pointing due to torque imbalance created by the propulsion and coupled thrusters.

## 2.2. Orbit, Attitude and Maneuvers

The orbit of Metop has a repeat cycle of 29 days and operates at an altitude of approximately 826 km. In-plane maneuvers are performed to keep the ground track to within ±5 km of the reference ground track and to satisfy the frozen eccentricity condition. During low solar activity, approximately two IP maneuvers are performed every year. When the Sun is active, the number may increase to four. Nevertheless, the maneuver frequency can also be influenced by the performance of the thrusters.

For inclination correction, OOP maneuver is performed to maintain the the Local Time of the Ascending Node (LTAN) offset to within two minutes of 21h 30min. This inclination control keeps the spacecraft in its Sun synchronous orbit. In general, the Metop spacecraft requires a correction to the inclination once every 18 months. When the inclination change maneuver requires longer than the allowed time when the satellite is in eclipse, a double OOP maneuver with a time separation of one or two weeks may occur. In October 2014 the inclination correction of 62.5 mdeg for Metop-B was performed in two burns with a time separation of 2 weeks.

The AOCS uses the Sun sensor for yaw control, the Earth sensor for pitch and roll control, and two bi-axial gyros for coherency monitoring [2]. During the LIP and OOP maneuvers, the spacecraft attitude is automatically controlled using the attitude and coupled thrusters as commanded by the AOCS. The SIP maneuvers are executed in the YSM whereas the LIP and OOP are performed after the spacecraft has transitioned to the FPM. This attitude mode is equivalent to the nominal attitude pointing or geocentric pointing. As for the SIP maneuver, the AOCS automatically activates the attitude thrusters to correct the yaw-steering attitude pointing after the main burn terminates. These attitude corrective/stabilization thrust pulses can last up to 6 minutes. Attitude stabilization also applies to LIP maneuvers. It occurs after the main burn to re-establish the FPM before transitioning back to YSM guidance.

The execution of OOP maneuvers is restricted to periods when the spacecraft is in eclipse. This is to protect the scientific instruments from exposure to the Sun when the spacecraft is performing the slew and anti-slew maneuvers [3]. Prior to the slew maneuver, the spacecraft changes its attitude guidance law from YSM to FPM. The attitude mode transitions to and out of FPM occur when the spacecraft is close to the poles where the yaw angle aligns very closely with the in-flight velocity direction. This is to avoid any transient motion due to the guidance law change [2]. Thereafter, the spacecraft is slewed to align the propulsion thrusters in the direction normal to the flight direction. Upon completion of the OOP thrust phase, the anti-slew maneuvers are commanded to return to the nominal flight configuration. The commanded slew and anti-slew angles always account for the yaw angle offset of the propulsion plates with respect to the flight direction. The mounting offset is approximately 10° and 20° in the velocity and anti-velocity direction, respectively [3]. Thus the rotation is always higher than 90° in the slew and anti-slew maneuvers. A graphical representation of an OOP maneuver sequence is demonstrated in Fig. 2. It is a generic representation and thus the slew and anti-slew rotation angle is not drawn to scale. The transition from FPM to YSM guidance after the maneuver may occur half an orbit later.

## 3. Flight Operations

This section of the paper provides a brief overview of maneuver planning and post maneuver activities that complements the maneuver calibration performed in the POD, and is not meant to be exhaustive. The details of the planning involving maneuver prediction, methodology used and generation of maneuver tele-commands can be found in [3]. In preparation for a maneuver, the flight dynamics team derives from its trajectory analysis the maneuver parameters and attitude guidance transition commands. The latter is only necessary for LIP and OOP maneuvers. The total required net force, as computed in the maneuver planning, to change the course of the trajectory is translated to the total number of thrust pulses required. The spacecraft recognizes, at the minimum, the start time of the maneuver and the number of pulses required in executing the maneuver. The LIP and OOP maneuvers require additional commands to change the guidance law from YSM to FPM and then back after the thrust phase. This primarily involves the time of the attitude mode transition. In addition to that, the OOP maneuver requires the command to start the slew and anti-slew to properly align the propulsion thrusters in the direction normal to the velocity, and the slew angle desired. The onboard AOCS continuously monitors and controls the attitude evolution to satisfy the commanded requirements. Aside from the propulsion thrusters being active during the OOP maneuver, the other four attitude thrusters are also actively commanded by the AOCS to maintain the FPM attitude pointing throughout the maneuver phase.

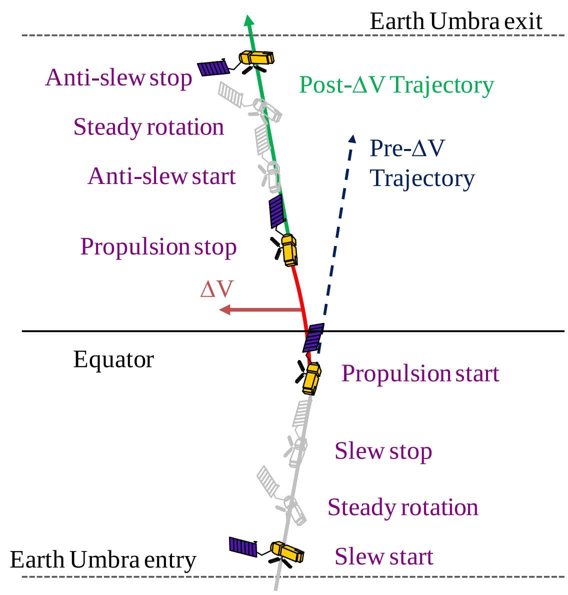


**Figure 2 Generic representation of Metop out-of-plane maneuver sequence**

For the purpose of maneuver calibration, the maneuver segments are reconstructed based on information retrieved from the spacecraft telemetry. The thrust for each segment is the integration of the forces produced by the number of pulses within the thrusting phase. It should be noted that the spacecraft telemetry records the thrust pulse at 1 Hz and each thruster activates independently from the other as commanded by the onboard AOCS.

Aside from the thrust information, the spacecraft attitude profile during the maneuver phase can also be retrieved from the telemetry. This is especially necessary for accurate OOP maneuver calibration as it is not possible to reconstruct the attitude model otherwise. This direct retrieval offers a straight-forward and simple method to reconstruct the real attitude model. It is also a very economic method compared to developing an attitude determination software tool.

## 4. Maneuver Calibration History and the Anomaly

The past calibrations of OOP maneuvers for both Metop satellites are performed without accurate attitude knowledge in the POD during the thrust phase. Both the GPS pseudorange and carrier phase measurements are used in the calibration. Even when the accuracy of the calibrated maneuvers is less reliable due to low observability (in the measurement sense) within the thrust phase, the consistency in the precision of the calibrated maneuvers is considered a valuable merit in identifying anomalies in the process. The statistics collated from the last three calibrations are tabulated in Tab. 2 and Tab. 3. The data editing criteria in the POD are set very loose in all calibrations.

**Table 2. Summary of past calibrated OOP maneuvers for Metop-A**

| Maneuver (m/s) Angle (°) | Mar 21, 2013 | | | Mar 26, 2014 | | | Apr 9, 2014 | | |
|---|---|---|---|---|---|---|---|---|---|
| | FD | POD | Δ | FD | POD | Δ | FD | POD | Δ |
| *Slew + Anti-Slew* | | | | | | | | | |
| Radial | -0.0410 | -0.0407 | 0.0003 | -0.0410 | -0.0374 | 0.0036 | -0.041 | -0.0355 | 0.0055 |
| Along-track | -0.0960 | -0.0981 | -0.0021 | -0.0960 | -0.0971 | -0.0011 | -0.096 | -0.0972 | -0.0012 |
| Cross-track | -0.0650 | -0.0683 | -0.0033 | -0.0650 | -0.0676 | -0.0026 | -0.065 | -0.0702 | -0.0052 |
| *Main OOP* | | | | | | | | | |
| Radial | -0.1747 | -0.1696 | 0.0051 | -0.1530 | -0.1548 | -0.0018 | -0.1659 | -0.1700 | -0.0041 |
| Along-track | -0.2668 | -0.2648 | 0.0020 | 0.1651 | 0.1663 | 0.0012 | 0.1151 | 0.1163 | 0.0012 |
| Cross-track | 4.5312 | 4.5352 | 0.0009 | 4.1512 | 4.1546 | 0.0034 | 4.4805 | 4.4857 | 0.0052 |
| OOP Thrust angle | 93.370 | 93.343 | -0.027 | 87.723 | 87.708 | -0.015 | 88.528 | 88.515 | -0.013 |

The column with the abbreviation 'FD' signifies values as provided by the Flight Dynamics team. The delta-v contributions from the slew and anti-slew maneuvers from FD are the theoretical values while the OOP main burns are estimated based on ranging and Doppler data. The column 'POD' implies the delta-v estimated in the POD using GPS phase and pseudorange measurements. The delta-v deviation of the POD from the FD is also shown in the column in blue. The OOP thrust angle relative to the flight direction is also computed and specified in the last row of each table.

**Table 3. Summary of past calibrated OOP maneuvers for Metop-B**

| Maneuver (m/s) Angle (°) | Nov 5, 2013 | | | Oct 8, 2014 | | | Oct 22, 2014 | | |
|---|---|---|---|---|---|---|---|---|---|
| | FD | POD | Δ | FD | POD | Δ | FD | POD | Δ |
| *Slew + Anti-Slew* | | | | | | | | | |
| Radial | -0.0410 | -0.0320 | 0.0090 | -0.0410 | -0.0357 | 0.0053 | -0.041 | -0.0336 | 0.0074 |
| Along-track | -0.0960 | -0.0984 | -0.0024 | -0.0960 | -0.1080 | **-0.0120** | -0.096 | -0.1064 | **-0.0104** |
| Cross-track | -0.0650 | -0.0605 | 0.0045 | -0.0650 | -0.0602 | 0.0048 | -0.065 | -0.0668 | -0.0018 |
| *Main OOP* | | | | | | | | | |
| Radial | -0.2035 | -0.2175 | -0.0140 | -0.2042 | -0.2120 | -0.0078 | -0.1921 | -0.2042 | -0.0121 |
| Along-track | 0.1722 | 0.1745 | 0.0023 | 0.1020 | 0.1140 | 0.0120 | 0.1897 | 0.1999 | 0.0102 |
| Cross-track | 4.2922 | 4.2874 | -0.0048 | 4.2639 | 4.2608 | -0.0031 | 4.0769 | 4.0777 | 0.0008 |
| OOP Thrust angle | 87.803 | 87.670 | -0.033 | 88.630 | 88.467 | **-0.162** | 87.336 | 87.194 | **-0.143** |

The variation in the along-track differences, Δ (column in blue), from the combined slew and anti-slew maneuvers in all three calibrations for Metop-A is relatively precise and close to what is expected. The cross-track acceleration contribution is relatively small compared to the contribution from the main OOP burn which is not of interest in this analysis. The focus is primarily on the along-track component. While the estimation of the acceleration contribution in this component is relatively precise for Metop-A, the estimates for Metop-B seem to deviate quite radically in the last two calibrations. This deviation is approximately one significant digit larger than Metop-A values. It is these two anomalies that prompt the refinement of the orbit modeling in the POD to better understand the source of this discrepancy.

## 5. Precise Orbit Determination

This section is dedicated to the description of the calibration of the multi-segment maneuver in the POD, the models used and the processing methodology. The software package used in this analysis is ESOC/ESA NAPEOS (Navigation Package for Earth Observation Satellites). NAPEOS is designed for orbit determination/prediction, maneuver planning and point positioning using various measurement data types. When modeling the Metop orbit in this analysis, an attitude profile is generated using an independent software tool that ingests attitude information as retrieved from the telemetry. This enables accurate attitude modeling in the POD during the OOP maneuver. In addition, the thrust model is reconstructed based on telemetry information and set as a-priori/commanded values. The reconstructed attitude model is the primary difference between this analysis and the nominal maneuver calibration process in the POD for Metop.

### 5.1. Attitude Model

In constructing the attitude model during the OOP maneuver phase, the roll, pitch and yaw angle deviations are assumed to be zero during FPM. The spacecraft switches from using the reaction wheels and magneto-torquers to attitude thrusters prior to the start of the slew maneuver. At this point of transition, the yaw angle deviation is retrieved from the telemetry. The sampling rate of the retrieved yaw angle is approximately 16 seconds. The roll and pitch angle deviations, during this phase, are much smaller than the yaw angle and are therefore neglected. The telemetry derived yaw angles remain valid until moments after the end of the anti-slew maneuver when the spacecraft resumes attitude control using reaction wheels and magneto-torquers [3].

A dedicated software tool has been developed to generate a continuous attitude profile for OOP maneuver calibration in the POD. This software tool is dependent on existing NAPEOS software modules. The attitude profile generation tool takes as input the mode transition times, the telemetry derived yaw angle data and a coarse orbit of the satellite. The reconstructed attitude profile for a processing arc is a combination of three different profiles; namely YSM, FPM and telemetry-derived yaw angle deviation. In the yaw-steering mode, the angles are computed according to Eq. 1[4].

$$\begin{aligned} roll &= -e^2 \cdot \frac{a_e}{a} \cdot \sin i \cdot \cos i \cdot \sin u \\ pitch &= -e^2 \cdot \frac{a_e}{a} \cdot \frac{\sin^2 i}{2} \cdot \sin(2u) \\ yaw &= \arctan\left( \frac{\sin i \cdot \cos u}{\frac{\omega_0}{\omega_e} - \cos i} \right) \end{aligned} \tag{1}$$

where:

| | |
|---|---|
| $u$ | Argument of latitude |
| $e$ | Eccentricity of the Earth reference ellipsoid |
| $a_e$ | Semi-major axis of Earth reference ellipsoid |
| $a$ | Mean semi-major axis of the satellite reference orbit |
| $i$ | Mean inclination of the satellite orbit |
| $\omega_0$ | Angular rate of the rotation of the Earth |
| $\omega_e$ | Angular velocity of the satellite |

The model for Metop-B generated for October 8, 2014 is illustrated in Fig. 2. The figure on the right is a zoom-in of the profile on the left. The transition from YSM to FPM can be clearly distinguished by the change to achieve a constant zero yaw angle. The OOP maneuver phase is bracketed by the two vertical dashed lines. The guidance mode transition times occur close to the pole crossings. The actual times of the transitions are tabulated in Tab. 4. The maneuver phase start and stop times are approximately 13:07:22.272 and 13:37:32.000 UTC, respectively. Within this phase, the attitude thrusters are used for attitude control and the propulsion thruster (T13/T15) for providing the actual OOP thrust. In this analysis, the attitude profile for the maneuver phase is generated at 10 seconds interval which is equivalent to the data sampling used in the POD. The yaw angle values at the required epochs are linearly interpolated between two telemetry points. The roll and pitch deviation angles are assumed to be very close to zero and their slight deviation would not have significant impact on the orbit estimation.

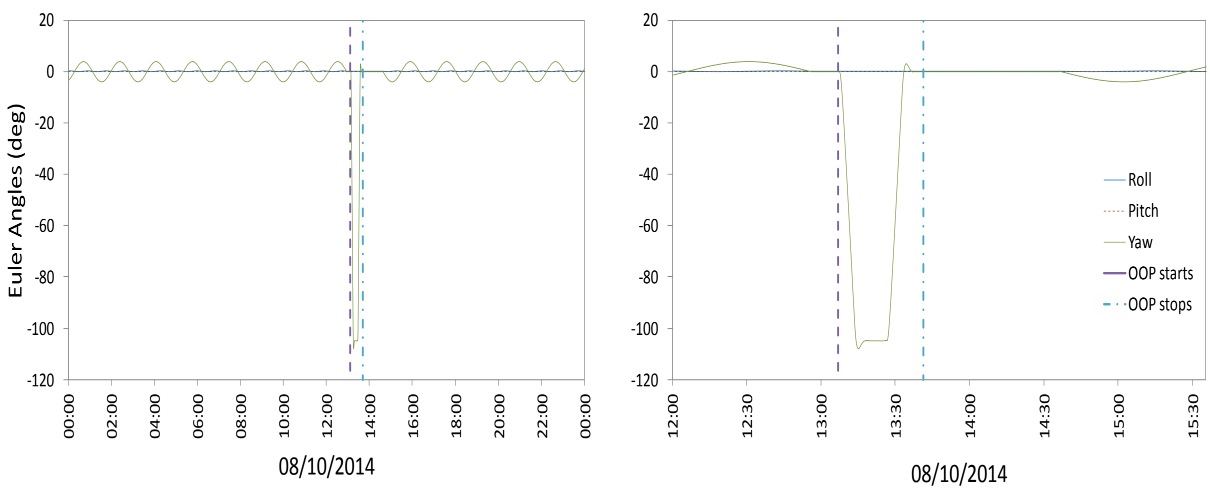


**Figure 3 Metop-B reconstructed attitude profile on October 8, 2014**

**Table 4 Timeline of Metop-B guidance mode transitions on October 8, 2014**

| Mode Transition | Epoch (UTC) |
|---|---|
| YSM $\rightarrow$FPM | 12:56:21.254 |
| FPM$\rightarrow$YSM | 14:37:08.243 |

### 5.2 Thrust Segment Modeling

The thrust segments that are used as a-priori values in the POD are reconstructed from integrating the force asserted by the total thrust observed in the telemetry. Figure 4 shows the total number of thrust pulses for each thrust segment. According to the recorded counter, a total of more than 8000 pulses are activated for the OOP maneuver on October 8, 2014. The figure is based on data sampled at 2 seconds and each second can accommodate up to 8 pulses per thruster. For the times when the pulse/sample is less than 16, it implies that the thruster is not firing at 8Hz per second.

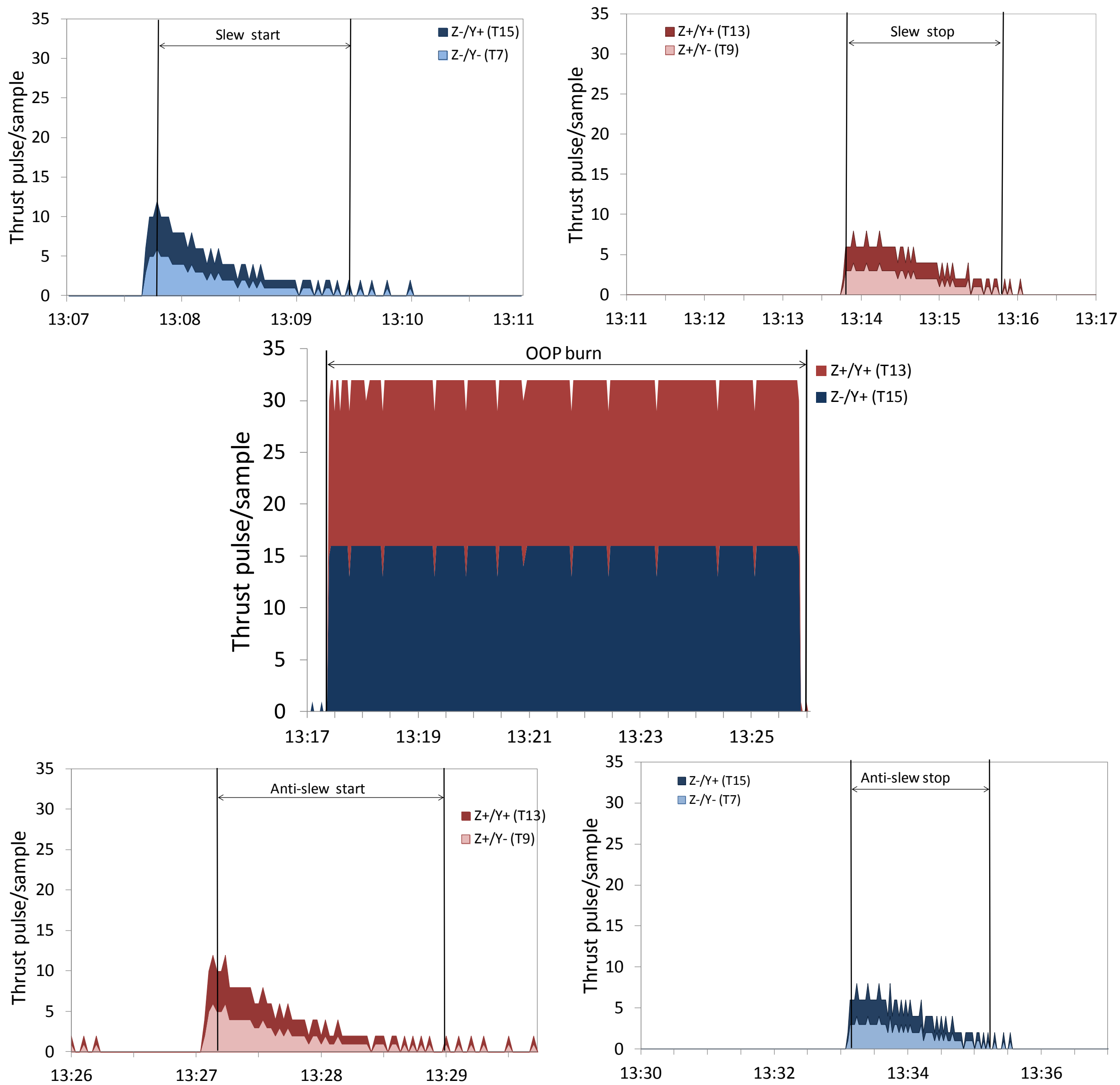


**Figure 4 Thrust profile of each maneuver segment from the propulsive/coupled thrusters**

The factors that may impact the maneuver calibration performance in the POD is the exact start and stops times of each segment, and a constant thrust that is assumed within each thrust segment. The details of the slew and anti-slew characterization are provided in [3] and will not be repeated here. The focus of this paper will be primarily on the exploitation of the thrust information as derived from telemetry data in the POD. This aids in fine tuning the thrust segments and the times associated to each maneuver.

Figure 4 is a stacked plot of the pulses contributed by the coupled and propulsion thrusters that are active within the time frame. The thrust segment is indicated by the black solid vertical lines. The period with the most significant thruster activity is evidently the main OOP propulsion which is the third segment (middle) shown in the figure. It is evident that the derived times of each maneuver segment do not necessary start exactly at the start time of the pulse activation. The pulses that occur outside of the segment window are currently not taken into account in the POD. Based on the complexity of the thrust pulse signatures as seen in the figure, it would require meticulous handling of the thrust model to care for all the external forces. This will without doubt require more number of segments and each of these segments will be relatively small.

When referring to the OOP thrust profile (middle), the irregular drop in the pulsation shows that the thrusters are responding to the torque imbalance by reducing the number of pulses in one thruster. The thrust exerted on the spacecraft in each orbit component is presented in Fig. 5. It complements the top and bottom sub-figures of Fig. 4. The left of Fig. 5 represents the slew and the right describes the anti-slew. The peaks in the time series are indications of the start and stop slew/anti-slew maneuvers. The thrust for each maneuver segment is computed with the aid of the information provided in Fig. 5.

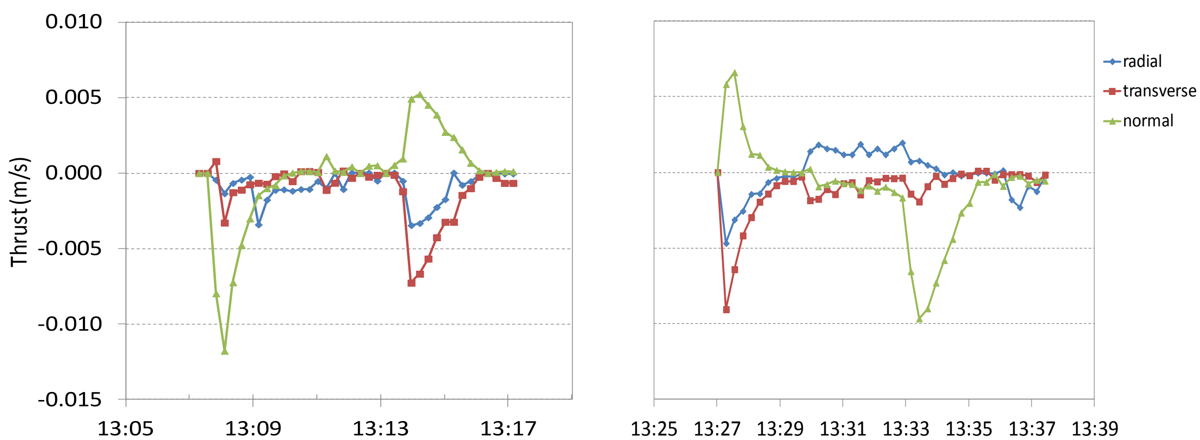


**Figure 5 Accumulated thrust profile during the slew (left) and anti-slew (right) maneuvers**

Even within the maneuver segments, the attitude control thrusters are actively stabilizing the attitude pointing. The thrust profile for each attitude control thruster is presented in Fig. 6. The shaded grey area indicates the five maneuver segments. The y-axis represents the number of pulses per sample, the same as shown in Fig. 4. Note that the AOCS can also command the propulsion/coupled thrusters to control the attitude pointing throughout the maneuver phase. However, no effort is made at the moment in reconstructing the thrust (if any) imposed by the attitude thrusters on the spacecraft in between the maneuver segments. It is important to note that the attitude control thrust pulses, which fall within the maneuver interval, are taken into account when reconstructing the five maneuver segments.

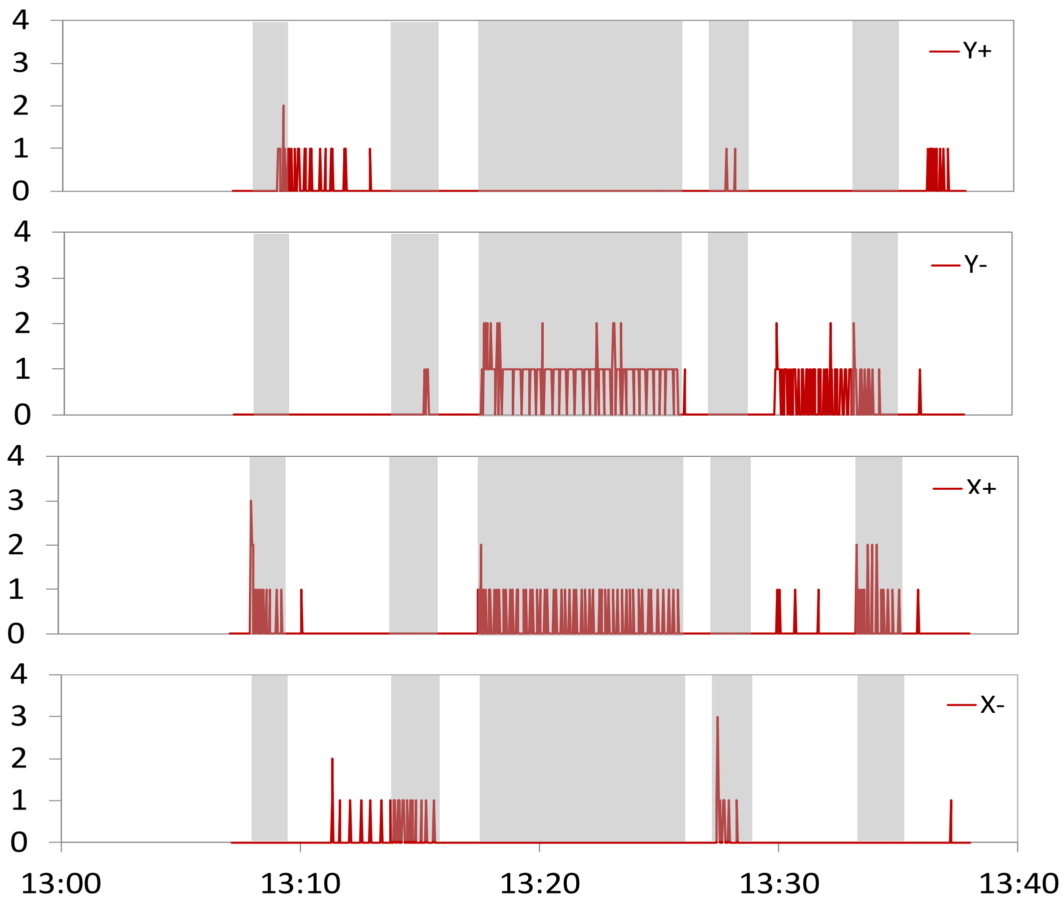


**Figure 6 Thrust profile from the attitude control thrusters**

### 5.3 Dynamical and Measurement Models, and Processing Strategy

The POD models used in this analysis are summarized in Tab. 5. The Metop-B orbit and maneuvers are estimated using GPS measurements from the GRAS instrument. The GPS orbits and clocks are the final operational product generated by AIUB with the clocks sampled at 30s interval. Since the processing uses a higher rate of 10s, the clocks are interpolated to 10s. GPS measurement below the elevation cut-off angle of 7˚ are not included in the processing and no elevation dependent weighting is applied to measurements above the cut-off angle when computing the statistics for data editing. The GPS and GRAS antenna phase center offsets (PCO) and variations (PCV) are applied. The GPS PCO and PCV are obtained from the International GNSS Service (IGS) while the GRAS PCO and PCV are the original values as provided by industry. The location of the GRAS antenna on Metop is marked with a red circle as shown in Fig. 7.

The parameters that are estimated consists of the spacecraft state vector, sine and cosine one cycle per revolution (CPR) empirical acceleration coefficients in the along-track and cross-track components, the drag coefficient, the receiver clock bias, the float GPS phase ambiguity and the maneuver in the three orbit components. The GPS phase bias parameter is only estimated if phase measurements are used in the processing.

When reconstructing the thrust segments, the changes in mass and pressure tanks are accounted for after the slew and OOP maneuvers. The satellite mass change is not taken into account after each maneuver in the POD. The values used are based on those before the start of the maneuver. In the POD, each maneuver is treated as a constant continuous acceleration in the three orbit components in NAPEOS. The existence of a maneuver implies a discontinuity in the modeling as the numerical integrator is restarted at the start and end of the maneuver. The estimation of the thrust or delta-v is constrained by two parameters: the percentage of uncertainty in the *a-priori* acceleration and the acceleration sigma.

**Table 5 Summary of the models used in the POD for OOP maneuver calibration**

| | |
|---|---|
| *Reference system* | |
| Polar motion and UT1 | IERS2003 |
| GPS orbits and clocks | COD final operational products<br>*Clocks at 30s interval* |
| Earth Orientation Parameters | IERS EOP series |
| Satellite reference | External attitude file |
| *Gravitational Forces* | |
| Gravity field model | EIGEN-GL04C (120x120) |
| Solid-Earth, pole and ocean tides | IERS2003, Topex 3.0 |
| Third body | JPL DE-200 |
| *Non-gravitational Forces* | |
| Solar radiation pressure | Cannonball with $C_R = 1.0$ |
| Earth radiation | Albedo and infra-red applied |
| Atmospheric density model | MSIS-90 |
| *Empirical accelerations* | |
| Drag coefficients | 5 per day |
| 1/rev sin and cos coefficients | 2 sets per day in along- and cross-track directions |
| Maneuvers | |
| Error in acceleration knowledge | 1% |
| Acceleration sigma | 3% |
| GPS measurements | |
| Sampling | 10s |
| Elevation cut-off angle | 7° |
| Elevation dependent weighting | No |
| Measurement weighting | 1 cm (phase), 1 m (pseudorange) |
| Antenna phase center | Offset and variations applied |
| Phase wind-up | Applied |
| Receiver clock | Bias estimated per epoch |
| Phase ambiguity | Float ambiguity estimated per pass |

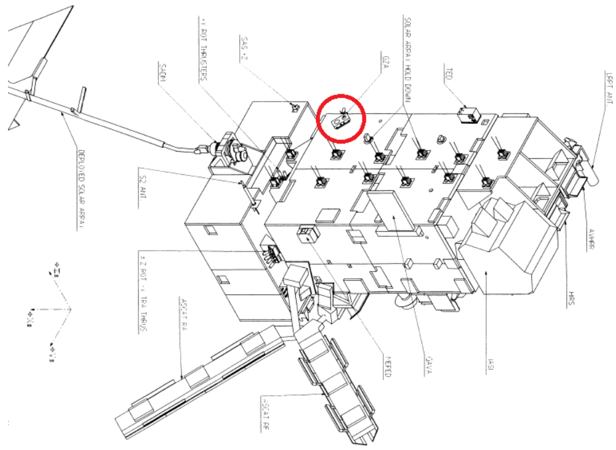

**Figure 7 Location of the GRAS navigation antenna on Metop**

## 5.4 Processing Scenarios

The analysis performed in this study comprises three scenarios. The first is the case in which the nominal attitude (YSM) is used even during OOP maneuver phase. This serves as a reference to validate the impact of the refined and reconstructed attitude model in the POD. The five reconstructed maneuver segments (slew start, slew stop, main burn, anti-slew start and anti-slew stop) are estimated in all scenarios. The second scenario uses the reconstructed attitude model based on telemetry data and YSM. The third uses only the pseudorange measurement and with accurate attitude knowledge. The data editing criteria for the first two scenarios is less stringent than the third. From this point onward, the three scenarios are tagged as follows for simplicity:

- Scenario A: Use of course attitude model; phase and pseudorange
- Scenario B: Use of reconstructed attitude model; phase and pseudorange
- Scenario C: Use of  reconstructed attitude model; pseudorange only

In order to provide the POD with a reference orbit, the geometrical positioning method is used to compute a coarse 3D position per epoch using only pseudorange measurements. The algorithm employs the Bancroft method which is robust in low Geometric Dilution of Precision (GDOP) situations and utilizes the least-squares approach for solving an over-determined system [5]. A positional accuracy at the decimeter level can be achieved with the Bancroft method. The computed Bancroft solution is then used in two separate processing: attitude reconstruction and POD.

For reconstructing the attitude profile, the Bancroft orbit solution is used in computing the yaw steering angle at the sub-satellite point when the satellite is in the YSM. In view of the low accuracy of the onboard orbit information in computing the yaw steering, the attitude difference between the on-board and Bancroft orbit solution is considered negligible. In fact, the Bancroft orbit solution provides a more accurate orbit solution.

For the POD, the Bancroft solution is smoothed with the aid of a dynamical orbit model in NAPEOS. This smoothed solution then serves as an initial/*a-priori* orbit in the POD. In scenarios A and B, the ionosphere-free phase residuals from the POD offer a simplistic technique to assess the thrust and attitude modeling, and the impact of the attitude knowledge on the overall maneuver calibration.

## 6. Maneuver Calibration Performance Assessment

The performance of the maneuver calibration in the POD can be deduced by assessing the ionosphere-free GPS phase residuals during the OOP maneuver phase. The carrier phase measurement is able to provide highly precise positioning information when the correct integer phase ambiguity can be determined. In this analysis, the phase ambuiguities are estimated as float solution and not resolved to their integer values. Nevertheless, the float ambuiguity is still capable of providing centimeter or even millimeter level satellite position/orbit accuracy. Therefore, any mis-modeling in the thrust segment or/and in the attitude model can be clearly observed in the phase residuals. However, it may be not be easy to clearly distinguish between the different error sources.

In order to see the impact of the reconstructed attitude model in the calibration, the phase residuals from scenario A is first presented. Figure 8 shows the phase residuals that bracket the maneuver time frame. It is evident that the computed orbit model could not match closely with the measured phase model. The orbit computation assumes that the satellite is in YSM throughout the maneuver phase. The rejected measurements are indicated in red and the accepted in blue. The percentage of observations accepted in the processing within the interval shown in Fig. 8 is approximately 41%. The mis-modeling in the POD has created several sections with data gaps rendering the maneuvers and orbit in those parts unobservable.

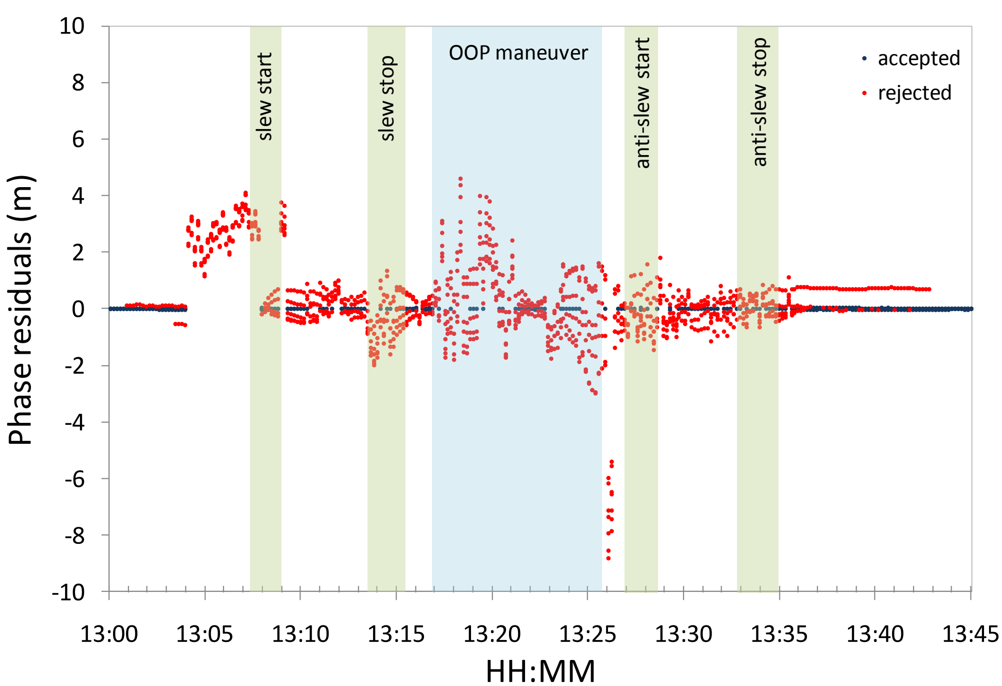


**Figure 8 Ionosphere-free phase residuals without accurate attitude knowledge for Metop-B on October 8, 2014**

The shaded areas indicate the five segments of maneuver with each color representing the slew/anti-slew and the OOP thrust. The large mismatch in the observed minus computed orbit can be attributed to the attitude knowledge, the assumptions made when reconstructing the thrust segments, and the fact that each thrust segment is modeled as a single continuous burn in the POD while neglecting any attitude deviation caused by the attitude control thruster/s.

As for the intervals in between maneuvers, the one factor of the phase deviation is the parasitic thrust that may have been exerted by the attitude control thrusters in stabilizing the spacecraft. This statement is made in relation to the attitude thrust profile shown in Fig. 6. However, further analysis will be required to substantiate this claim. Other possibilities include the inaccuracy in the maneuver times and the un-modeled forces from the thrusters that occur outside the defined maneuver segments (refer to Fig. 4).

While it is easy to identify the approximate start time of the maneuvers, it is not so for the stop time for the slew and anti-slew maneuvers as shown in Fig. 4. For the purpose of flight dynamics operations planning, accurate modeling of the thrust segments is not of great importance. In fact, the calibrated results obtained solely from the pseudorange measurement without an accurate attitude model are sufficient. The advantage of scenario C is that the pseudorange-based calibrated maneuvers are fully observable even though the pseudorange measurement is less precise than the carrier phase.

When accurate attitude knowledge is considered in the POD, the phase residuals exhibit noticeable improvement as can be seen in Fig. 9. With the GRAS antenna located off the center of mass of the spacecraft, an accurate knowledge of the attitude knowledge is evidently beneficial. The dotted black line on the left indicates the time when the attitude thrusters are

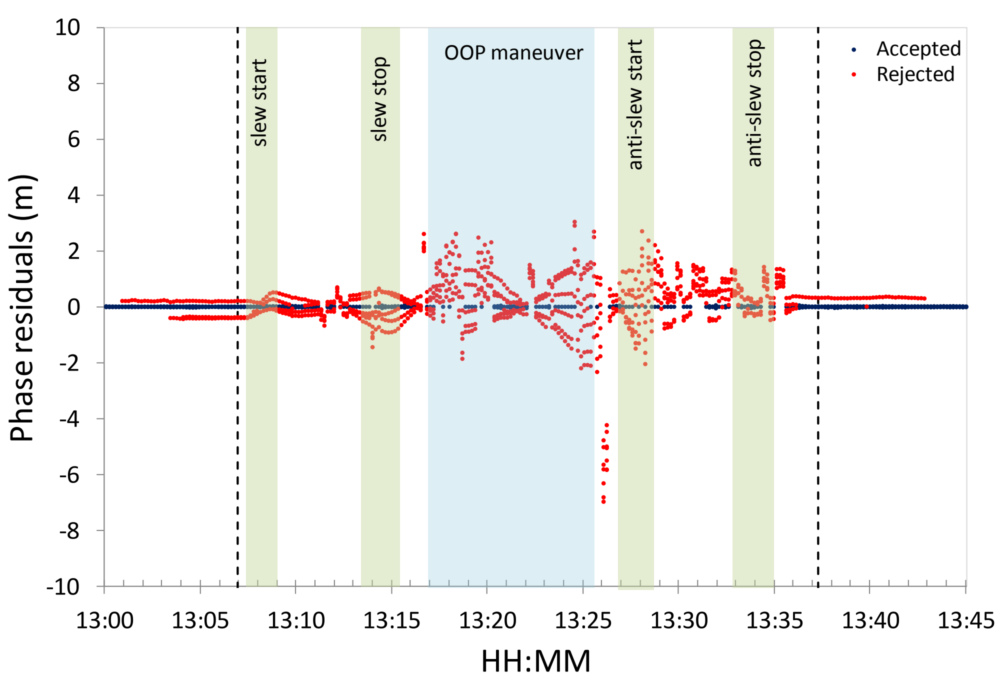


**Figure 9 Ionosphere-free phase residuals with reconstructed attitude knowledge for Metop-B on October 8, 2014**

commanded to replace the reaction wheels and magneto-torquers as attitude controller. After the maneuver is complete, the attitude thrusters are deactivated and the reaction wheels restored. The time of this swap is indicated by the dotted black line on the right.

If the above statement is taken into account, the large deviation in the phase residuals before and after the attitude control swap cannot be attributed to thruster activity. It may still be caused by inaccuracies in the attitude model as it is assumed that the FPM is perfect in the reconstructed attitude model. However, it is highly unlikely that the attitude deviation is significant enough to prompt such an impact on the orbit estimation. Another possibility is the inaccuracy in the time of the slew start maneuver. This point is evident when referring to Fig. 4. Fine tuning of the maneuver times would be required to further improve the performance of the calibration. Every effect has to be carefully accounted for when processing phase measurements in the POD in order to obtain the most accurate solution.

As mentioned earlier, scenario C involves a POD using only pseudorange measurements. In general, the accuracy from the pseudorange-calibrated maneuvers is sufficient for flight dynamics operations planning even with coarse attitude knowledge. Now that an accurate attitude model is available, it is of interest to assess the performance of this calibration. Thus the results are also included here as reference. Table 6 summarizes the overall statistics of the scenarios described. The *a-priori* OOP maneuver values used are derived from the telemetry while the slew/anti-slew are based on values obtained from Metop-A, which conforms to the theoretical values. The results shown for each scenario consist of the estimated delta-v and the percentage of accepted measurements in each processing.

The computed delta-v for each orbit component is shown separately for each maneuver type. One can relate the reliability of the computed delta-v with the percentage of measurements used in the estimation. In cases such as this whereby each segment of the maneuver is relative close to the other, the uncertainty in the estimation from the segment before can have significant impact on subsequent maneuver estimates. If the maneuver gaps (those in between maneuver segments) are without external disturbances and the orbit can be 'observed', it might have helped mitigate the error in the estimated orbit and maneuvers. Unfortunately these maneuver gaps are affected by constant thrust activity used in stabilizing the spacecraft. This is evident in the evolution of the percentage of observations accepted in each maneuver segment in scenario B. When comparing with scenario A, the total number of observation processed has doubled in the first maneuver. However the improvement is reduced in subsequent maneuvers. Overall, having a better knowledge of the attitude in the calibration does show noticeable improvement. One can conclude that the computed delta-v in scenario B is more accurate than those in scenario A. In order to further improve on the calibration performance, the thrust effect in between the maneuver segments has to be modeled and estimated in the POD.

Even with the slight disadvantage of the pseudorange-calibrated maneuvers, the observability of the maneuvers is exceptional based on the percentage of accepted observations (above 95%) in all segments. Given the results of scenarios B and C, and knowing the advantages and disadvantages of each, it is believed that the real maneuver values most likely fall in between the two numbers. Therefore, an average along-track delta-v contribution from the combined slew and anti-slew maneuvers is computed from scenarios B and C. Comparing this average value of -0.1019 m/s with the *a-priori*, it shows a deviation of -5.7 mm/s. In the case of Metop-A, the deviation from the *a-priori* is within ±2.6 mm/s. However, it should be noted that this deviation bracket is based on past calibrations without accurate attitude model. Nevertheless it is a good indication that a larger bias exists for Metop-B. As for the radial and cross-track components, the average deviations from the *a-priori* are +3.75 mm/s and -7.9 mm/s, respectively. For Metop-A, the radial delta-v has a mis-performance of +1.17 mm/s on the average and the cross-track component with a -2.67 mm/s average deviation. It is believed that the uncertainty in these deviations relate to the imperfect OOP main and anti-slew maneuver calibrations.

**Table 6 Summary of the calibrated maneuvers for Metop-B on 8 October 2014**

| Type | *A-priori* values | Course Attitude | | Reconstructed Attitude | | | |
|---|---|---|---|---|---|---|---|
| | | Scenario A | | Scenario B | | Scneario C | |
| | | Δv (m/s) | % acc. obs | Δv (m/s) | % acc. obs | Δv (m/s) | % acc. obs |
| *Residual slew* | | | | | | | |
| Radial | -0.0351 | -0.0101 | 16.67 | -0.0376 | 33.33 | -0.0325 | 97.10 |
| Along-track | -0.0451 | -0.0480 | | -0.0478 | | -0.0455 | |
| Cross-track | -0.0052 | 0.0005 | | -0.0004 | | 0.0060 | |
| *OOP thrust* | | | | | | | |
| Radial | -0.2042 | -0.2082 | 9.22 | -0.2067 | 13.13 | -0.2116 | 96.88 |
| Along-track | 0.1021 | 0.1099 | | 0.1092 | | 0.1059 | |
| Cross-track | 4.2639 | 4.2820 | | 4.2855 | | 4.2698 | |
| *Residual anti-slew* | | | | | | | |
| Radial | -0.0060 | -0.0073 | 13.68 | -0.0027 | 16.23 | -0.0019 | 98.47 |
| Along-track | -0.0512 | -0.0560 | | -0.0555 | | -0.0545 | |
| Cross-track | -0.0600 | -0.0788 | | -0.0803 | | -0.0716 | |
| *Slew+anti-slew* | | | | | | | |
| Radial | -0.0411 | -0.0386 | | -0.0403 | | -0.0344 | |
| Along-track | **-0.0962** | **-0.1040** | | **-0.1033** | | **-0.1000** | |
| Cross-track | -0.0652 | -0.0783 | | -0.0807 | | -0.0655 | |
| *Total* | | | | | | | |
| Radial | -0.2443 | -0.2468 | | -0.2470 | | -0.2460 | |
| Along-track | 0.0059 | 0.0059 | | 0.0059 | | 0.0059 | |
| Cross-track | 4.1987 | 4.2037 | | 4.2048 | | 4.2043 | |

An analytical computation of the net acceleration contribution from the slew and anti-slew maneuvers is also performed. The derivation is based on the 16Hz telemetry thrust profile and yields -0.0355 ms/, -0.0956 m/s and -0.0532 m/s in the radial, along-track and cross-track components, respectively. The thrust force used in the computation is the average force of the eight thrusters at the start of the maneuver; assuming each thruster has 100% efficiency. The satellite mass is the weight prior to the start of the maneuver and is kept as a constant in the entire computation. Even though there are independent means to assess the performance of the maneuver calibration, the uncertainties inherited in each method forbids a concrete conclusion be drawn. With the uncertainties still exist in the POD orbit modeling, the magnitude of the along-track acceleration discrepancy in the slew/anti-slew maneuvers cannot yet be fully justified at this point. Further refinement in the orbit modeling will be made as the next step.

## 7. Conclusion

An observed discrepancy in the along-track acceleration contribution from the slew and anti-slew maneuvers of Metop-B has prompted the development of an accurate attitude model to be used in the POD to improve the calibration of each maneuver segment. It is of importance to flight dynamics operations planning in understanding the actual contribution in acceleration by the slew and anti-slew maneuvers if an anomaly does exist between two Metop spacecraft that have the same design and assembly.

The performance of the maneuver calibration for each segment using the reconstructed and more accurate attitude model has shown noticeable improvement. The results from this analysis have provided a better indication of mis-performance of the slew and anti-slew maneuvers of Metop-B. Its along-track acceleration contribution is almost double the past calibrated slew/anti-slew maneuvers of Metop-A. For proper comparison and assessment, it is foreseen that all past OOP maneuvers for Metop-A and Metop-B will be calibrated using a reconstructed attitude model. If the mis-performance persists in all Metop-B OOP maneuvers, this may indicate a possible misalignment in the coupled thruster on Metop-B thus changing the direction of the parasitic accelerations. These accelerations contribution is observed in all three components of the orbit but it is the along-track component contribution that is of interest to flight operations planning. If a thruster mis-alignment is present, this will have to be taken into account in all future maneuver planning of Metop-B. With the experience gained from this analysis and the basic resources developed, future OOP maneuver calibration in the POD can be readily performed for the future Metop-C as well as the EPS-SG satellites to aid operations planning.

## 8. Future Work

The analysis undertaken thus far has shown very promising outcome by accounting for accurate modeling of the spacecraft attitude during the maneuver phase in the POD. It is foreseen that further improvement in the maneuver calibration performance can be achieved by including the following:

1) Fine tuning of the start and stop times of the maneuver segments
2) Modeling of the parasitic thrust effect caused by the attitude control thrusters in between the maneuver segments. This involves defining more smaller thrust segments
3) Divide the slew and anti-slew maneuvers into sub-segments to better represent the actual force exerted (Fig. 5)
4) Model the thrust, especially in the slew and anti-slew, as linearly increasing/decreasing variable acceleration over time.

The first three points are tasks that can be combined to produce the best results. The last point made is in relation to the force profile shown in Fig. 5. In order to manipulate this implementation in NAPEOS, small constant step-size thrust segments have to be developed. This is equivalent to the method described in 3) but with finer step-segments and are performed internally in the software during runtime. Needless to say, this will require modifications in the software algorithms to specifically handle such a thrust model.

## 9 Acknowledgements

The authors would like to acknowledge the Flight Dynamics team members at Eumetsat for providing the necessary information and clarification to make this analysis possible.

## 10. References

[1] Goody, N., "Metop Propulsion Subsystem User's Manual." MO-MA-MMB-SV-0517, Iss. 6, EADS Astrium, Hertfordshire, England, 2004.

[2] Garces, S., "Metop Space Vehicle Module Flight Operations Manual Volume 5 Ground Processing." MO.UM.MMT.SV.00004, Iss. 8, Rev. 7, 2013

[3] Sancho, F., Lazaro, D., Righetti, P.L., "Out-of-plane Manoeuvre Campaigns for Metop-A: Planning, Modelling, Calibration and Reconstruction." Proceedings 21$^{st}$ International Symposium on Space Flight Dynamics – 21$^{st}$ ISSFD. Toulouse, France, 2009

[4] European Space Agency, "MetOp Second Generation Space Segment: General Design and Interfaces Requirements." MOS-RS-ESA-SYS-0433, Iss. 1, Rev. 0, 2012

[5] Bancroft, S., "An Algebraic Solution of the GPS Equations." IEEE Transactions on Aerospace and Electronic Systems. Vol. AES-21, Iss. 1, pp. 56-59, 2013